HAL open science

Optical properties of Ni from 0.03 to 6 eV

M. Gadenne, J. Lafait

To cite this version:

M. Gadenne, J. Lafait. Optical properties of Ni from 0.03 to 6 eV. Journal de Physique, 1986, 47 (8), pp.1405-1410. 10.1051/jphys:019860047080140500 . jpa-00210334

HAL Id: jpa-00210334
https://hal.science/jpa-00210334

Submitted on 4 Feb 2008

HAL is a multi-disciplinary open access archive for the deposit and dissemination of scientific research documents, whether they are published or not. The documents may come from teaching and research institutions in France or abroad, or from public or private research centers.

L'archive ouverte pluridisciplinaire **HAL**, est destinée au dépôt et à la diffusion de documents scientifiques de niveau recherche, publiés ou non, émanant des établissements d'enseignement et de recherche français ou étrangers, des laboratoires publics ou privés.

J. Physique **47** (1986) 1405-1410 AOÛT **1986,** PAGE 1405

Classification
Physics Abstracts
78.65 – 78.20D

Optical properties of Ni from 0.03 to 6 eV

M. Gadenne and J. Lafait

Laboratoire d'Optique des Solides, U.A. au CNRS n° 040781, Université Pierre et Marie Curie, 4 place Jussieu, 75252 Paris Cedex 05, France

(*Reçu le 27 décembre 1985, révisé le 21 mars 1986, accepté le 16 avril 1986*)

Résumé. — La fonction diélectrique complexe de couches minces de nickel, déposées sur des substrats de silice fondue et de germanium, par évaporation thermique sous ultra-vide, est déduite de mesures optiques à l'aide de différentes méthodes : entre 6 et 0,5 eV à partir des mesures de réflexion et de transmission ; entre 0,5 et 0,09 eV par une méthode fondée sur la réflexion totale atténuée et l'excitation de plasmons de surface ; entre 0,2 et 0,03 eV *via* une analyse de Kramers-Kronig sur la réflectivité. Le seuil des transitions interbandes est ainsi déterminé et l'on calcule les paramètres de Drude des électrons de conduction. On discute les résultats en fonction des caractéristiques des couches (épaisseur, recuit, résistivité, taille des cristallites), et on les interprète à partir de calculs de structure de bande.

Abstract. — The complex dielectric function of Ni thin films deposited on fused silica and crystalline germanium substrates by thermal evaporation under ultra-high vacuum is deduced from optical measurements by various methods : from 6 to 0.5 eV from reflectance and transmittance measurements; from 0.5 to 0.09 eV by a method based on A.T.R. and surface plasmon excitation; from 0.2 to 0.03 eV by a Kramers-Kronig analysis performed on the reflectivity. The onset of interband transitions is thus determined and the Drude parameters of the conduction electrons are calculated. The results are discussed in relation to the characteristics of the films (thickness, annealing, resistivity, crystallites size) and eventually interpreted using band structure calculations.

1. Introduction.

The optical properties of transition metals are essentially governed by the position of the Fermi level, located within the d bands. In contrast to the noble metals, the onset of interband transitions is thus located at low energies. Consequently the Drude-like behaviour of the dielectric function can only be observed at very low energies. In the case of Ni, few optical measurements have been performed below 0.5 eV and most of the results concerning the dielectric function have been deduced from a Kramers-Kronig analysis of the reflectivity data, since they were obtained on polished bulk materials. These results, particularly the absolute value of the dielectric function, strongly depend on the conditions of preparation of the samples : electropolishing and annealing for bulk samples; vacuum, substrate temperature, annealing treatments for evaporated thin films. Moreover, due to the high infrared reflectivity of bulk Ni and its slow variations with energy or incidence, it is very difficult to deduce the infrared dielectric function from measurements on bulk samples with a good accuracy.

Consequently, we have studied the optical properties of both thin and thick Ni films condensed by thermal evaporation under ultra-high vacuum onto fused silica and crystalline germanium substrates, both as deposited and annealed. The crystallographic structure, the composition and the d.c. resistivity of the films have been determined. Their dielectric function has been deduced from three types of measurements in the 0.03 to 6 eV range :

— between 0.5 and 6 eV : reflectance and transmittance measurements on thin films;

— between 0.09 and 0.5 eV : attenuated total reflection (A.T.R.) measurements under oblique incidence, in the conditions of surface plasmon excitation;

— between 0.03 and 6 eV : reflectivity measurements on thick films, treated by Kramers-Kronig analysis.

The optical results are discussed as a function of the physical parameters of the films (thickness, crystallite size) and of the method of determination (direct resolution of Kramers-Kronig analysis).

The conduction electron parameters (plasma frequency ω_p and relaxation time τ) are deduced from the

Article published online by EDP Sciences and available at http://dx.doi.org/10.1051/jphys:01986004708014050

experimental dielectric function in the intraband range, using the Drude model. These parameters, as well as the location of the absorption edge and the main interband transition energies, are compared to the results obtained by other authors, and to recent band structure calculations.

Section 2 is devoted to the presentation of the optical techniques and the methods of calculation of the dielectric function. The A.T.R. method using surface plasmon excitation is described in detail. The preparation conditions and the main physical properties of the samples are given in section 3, while the optical results are discussed in section 4.

2. Optical methods and experimental set up.

2.1 NEAR-ULTRAVIOLET, VISIBLE AND NEAR-INFRARED RANGE (6 TO 0.5 eV). — The reflectance R and the transmittance T of thin semi-transparent films condensed on polished fused silica substrates have been measured under near-normal incidence using a Cary 17 spectrophotometer equiped with a Strong (V-W) attachment for absolute reflectivity measurements. Both the real and imaginary parts of the dielectric function $\tilde{\varepsilon} = \varepsilon_1 + i\varepsilon_2$ have been deduced from the experimental values of R and T using exact thin film formulae by an iterative implicit resolution procedure [1].

2.2 MIDDLE INFRARED RANGE (0.6 TO 0.09 eV). — Crystalline Ge, which is transparent in this spectral range, is used as a substrate material. The micro-roughness resulting from the optical polishing is larger for Ge than for fused silica; this results in slight differences in the Ni substrate interfaces, depending on the nature of the substrate. We show in the following that these differences do not affect considerably the dielectric function values.

Due to the relatively poor accuracy of the R and T spectrophotometric measurements in the infrared and the very high R values (close to 1) in the case under consideration, the method presented in 2.1 cannot be used. We used a method developed by Lafait [2], based on Attenuated Total Reflection under variable oblique incidence. Our aim is to obtain lower reflectivity values, sufficiently variable with the incidence and the wavelength to allow an accurate determination of ε_1 and ε_2. These requirements are fulfilled if a surface plasmon mode is excited at one of the interfaces of the thin metallic film.

This is achieved for the metal/air interface by using the Kretschmann configuration [3] (Fig. 1). If the reduced wave-vector is defined by $S = c/w_0.k_x$, where k_x is the longitudinal component of the wave vector, then, $S_1 = Re(S) = \varepsilon_0^{1/2}.\sin\phi_0$ and the condition for the surface plasmon excitation at the metal/air interface is given by :

$$\varepsilon_S/\sqrt{S^2 - \varepsilon_S} + \tilde{\varepsilon}/\sqrt{S^2 - \tilde{\varepsilon}} = 0 \quad \text{or} \quad S^2 = \varepsilon_S\,\tilde{\varepsilon}/(\varepsilon_S + \tilde{\varepsilon})$$

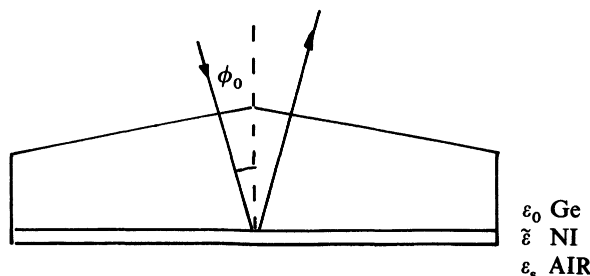

Fig. 1. — Kretschmann's configuration for surface plasmon excitation in thin films.

where ε_0, $\tilde{\varepsilon} = \varepsilon_1 + i\varepsilon_2$, ε_S are the dielectric functions of respectively the substrate (Ge), the metal and the air and ϕ_0 the angle of incidence at the substrate/metal interface. One has to notice that the p component (parallel to the plane of incidence) of the reflectance goes through a deep minimum at the plasmon resonance whereas the s component (perpendicular to the plane of incidence) is only weakly affected.

Since the real part, S_1, of the reduced wave vector S : $S_1 = 1 - (\varepsilon_0 + \varepsilon_1)/[(\varepsilon_0 + \varepsilon_1)^2 + \varepsilon_2^2]$ is close to 1 in transition metals, it is necessary to work near the critical angle ϕ_L ($\sin\phi_L = \varepsilon_0^{-1/2}$) for reflection in Ge. Moreover, the resonance can be clearly characterized in the reflectivity spectrum only if the damping due to the absorption is not important. The imaginary part S_2 of the wave vector S has thus to be much smaller than S_1. This condition is fulfilled by Ni at low energies ($S_1 \simeq 1$ and $S_2 \simeq 10^{-3}$). However, the remaining absorption sets a limit to the thickness of the film and prevents a perfect coupling of the p polarized incident wave to the plasma wave. The damping broadens the resonance minimum in the curve $R_p = f(\phi_0)$ and the reflectivity value does not completely vanish. The R_p variations beyond the critical angle of reflection ϕ_L, are however sufficient to allow an accurate determination of the dielectric function $\tilde{\varepsilon}$ by using a least-square fitting procedure with optimized gradient convergence, proposed by Bouchard [4].

The A.T.R. measurements have been performed on an infrared spectrophotometer, described in [2], built in our laboratory. The accuracy of the reflectivity measurements is about 0.01 and the angles of incidence, for this experiment, are varying from 14 to 16°. Figure 2 shows the R_p *versus* ϕ_0 experimental data as well as the results of the simulation for different energies. Figure 3 shows the R_p values as a function of ω for different angles of incidence.

2.3 EXTENDED MIDDLE INFRARED RANGE (0.5 TO 0.03 eV). — In order to extend the experimental energy range down to 0.03 eV and to compare the results obtained by the A.T.R. technique on thin films and by a Kramers-Kronig analysis of the reflectivity of thick films, we have deposited thick opaque films ($T < 10^{-4}$) on fused silica. Their reflectivity was

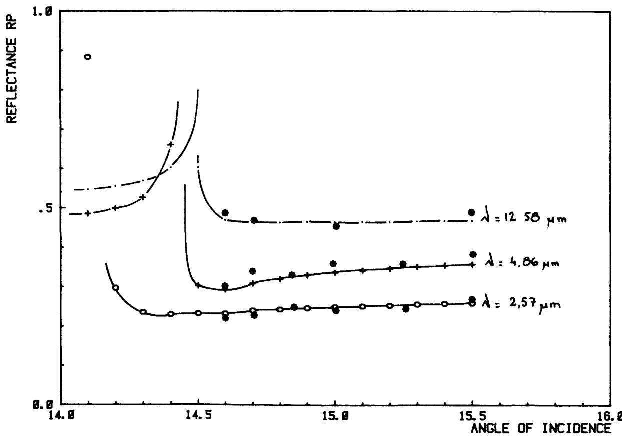

Fig. 2. — Variation of the reflectance R_p with the angle of incidence around the angle of resonance in Kretschmann's configuration for surface plasmon excitation in the case of Ni film (d = 320 Å thick). The dos .. crosses + and open circles O represent the calculated curves, respectively for λ = 12.58 μm, λ = 4.86 μm, λ = 2.57 μm and the stars represent the experimental data.

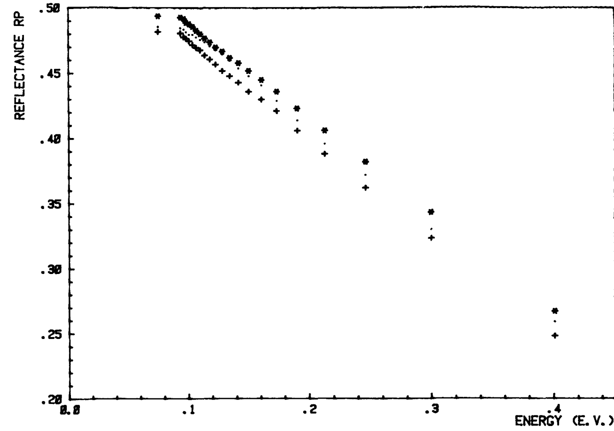

Fig. 3. — Variation of the reflectance R_p with the energy, for different angles of incidences : + — ϕ_0 = 14.7, . — ϕ_0 = 15 and * — ϕ_0 = 15.5.

measured in the 6 to 0.5 eV spectral range using a Cary 17 and in the 0.5 to 0.03 eV spectral range using a Perkin Elmer 580 B, both equiped with a Strong (V-W) attachment for absolute reflectivity measurements. The low energy extrapolation ($0 < \omega < 0.03$ eV) of the reflectivity, in the Kramers-Kronig integrals, has been taken equal to 1. We have used the classical extrapolation for high energies ($\omega > \omega_L$; ω_L = 6 eV)

$$R(\omega) = R(\omega_L).(\omega/\omega_L)^s$$

s being deduced from an $\tilde{\varepsilon}$ value determined on thin films in the 0.5 to 6 eV range (s = 1.47).

3. Sample preparation and physical characteristics.

The films have been deposited by flash-evaporation of Ni powder from a tungsten crucible, under ultrahigh vacuum (10^{-9} Torr) onto optically polished fused silica and crystalline germanium substrates. The d.c. resistance has been measured during the evaporation in order to control the film thickness, as well as during subsequent treatments. The thickness has been measured by X-ray interferences under grazing incidence (Kiessig method) with an accuracy of 1 %.

Electron diffraction and Rutherford backscattering studies confirm that we have crystalline Ni films free of contamination. Most of the samples have been annealed *in situ* up to 250 °C. After annealing, the temperature coefficient of the resistivity was found to be very close to the bulk one, but the resistivity values remain still higher than that of bulk Ni and can be directly related to the crystallite size (see Tab. I). In fact, the transmission electron microscopy studies show (see Fig. 4) that the films are made of small crystallites (200 to 600 Å), the size of which is not

Table I. — *Thickness d* (Å), *d.c. resistivity* (Ω cm) *and mean crystallite size of our* Ni *thin films.*

Sample	d(Å)	(μΩ cm) after annealing	Crystallite size (Å)
1	114	24.6	
2	275	10.9	600
3	320	11.3	
4	448	11.6	200
5	468	14.8	100
6	658	13.7	
bulk Ni	∞	6.8	

strongly affected by annealing but seems more dependent on the film thickness. The thinner the film, the larger the crystallites and the weaker the resistivity.

4. Optical results and discussion.

4.1 OPTICAL RESULTS, DIELECTRIC FUNCTION. — The optical results concerning the reflectivity and the dielectric function are presented in figures 5 and 6 respectively.

In order to compensate for the systematic small differences (1 to 2 percent) observed between the reflectivity measurements performed on the three apparatus, the data have been fitted in their common spectral range. This procedure does not affect the energies of the interband transitions. It may slightly shift the absorption onset, as it is pointed out by subtracting, from the total dielectric function, a Drude contribution calculated with these corrections.

We first compare three reflectance spectra corresponding to opaque films (Fig. 5) :

— one measured on a thick non annealed film;

— two calculated using the dielectric function determined by the methods described above on two thin annealed films with different crystallite sizes.

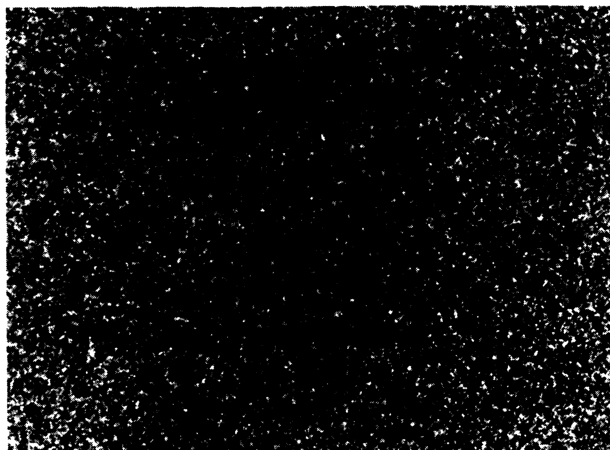

Fig. 4a.

1 μm

Fig. 4b.

Fig. 4. — Transmission electron micrographs. 4a : annealed film (d = 468 Å), crystallite size 200 Å. 4b : annealed film (d = 275 Å), crystallite size 600 Å.

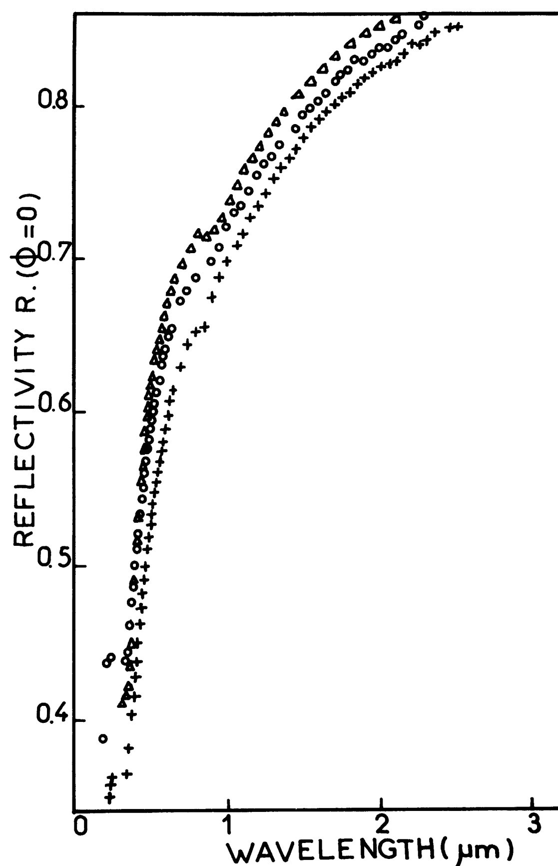

Fig. 5. — Spectral reflectivity corresponding to thick Ni. — + measured on thick non annealed evaporated film; — calculated, using the dielectric constant of thin annealed films ○ — with small crystallites; △ — with larger crystallites.

The highest values of the reflectivity are obtained with the dielectric function of the thin film with the largest crystallites : they are roughly two percent higher than those for the thin film with smaller crystallites, and four percent higher than the reflectivity of the thick non annealed film.

This result is in qualitative agreement with the correlations observed in 3 between the resistivity, the crystallite size and the film thickness.

Turning now to the complex dielectric function (Fig. 6), we observe a good agreement between the optical absorption curves ($\hbar\omega\varepsilon_2$) deduced from the Kramers-Kronig analysis, and from the direct determination by the R, T and A.T.R. methods. The latter are slightly higher in the infrared, confirming thus the weaker electrical resistivities observed on thin films with larger crystallites than on thick films with smaller ones. In both cases, the optical absorption bands corresponding to interband transitions are located at the same energies. We have plotted in figure 6, for memory, the results of Lynch *et al.* [5] obtained on a single crystal at low temperature, the absorption of which is lower as expected, and the results of Stoll [6], in complete agreement with ours.

4.2 Drude-like behaviour. — Due to the location of the Fermi level within the d bands of Ni, interband transitions still occur at low energies. The transition between pure intraband behaviour and mixed intraband-interband behaviour is clearly pointed out in an Argand diagram of $\omega\varepsilon_2$ *versus* ε_1 (Fig. 7) by the breakdown of the linear variation expected from the Drude model. The onset of interband transitions can thus be inferred to appear around 0.15 eV. Accordingly, we have calculated the Drude parameters of the conduction electrons from our experimental results in the estimated intraband region, i.e. below 0.15 eV.

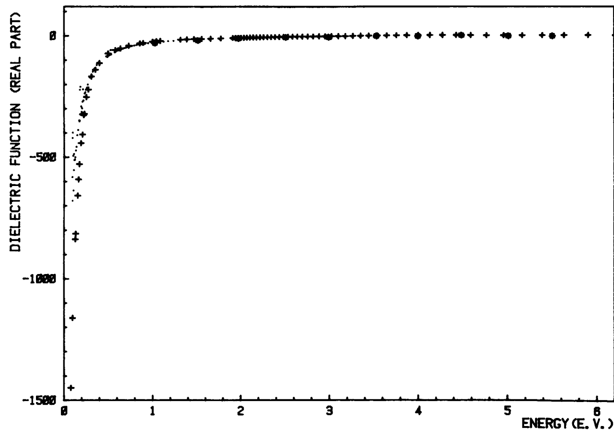

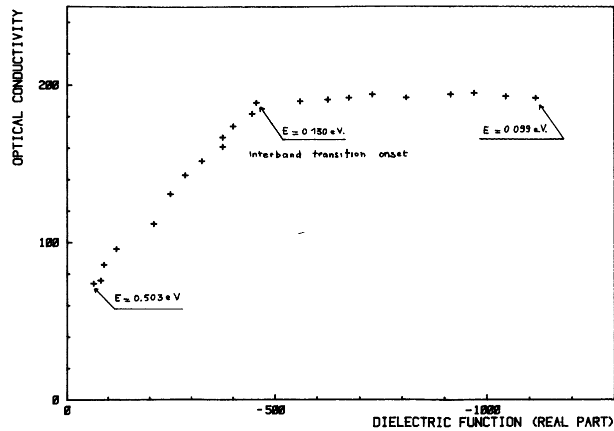

Fig. 7. — Argand diagram $\hbar\omega\varepsilon_2 = f(\varepsilon_1)$ for Ni. The results are obtained, by A.T.R. method, on a thin film.

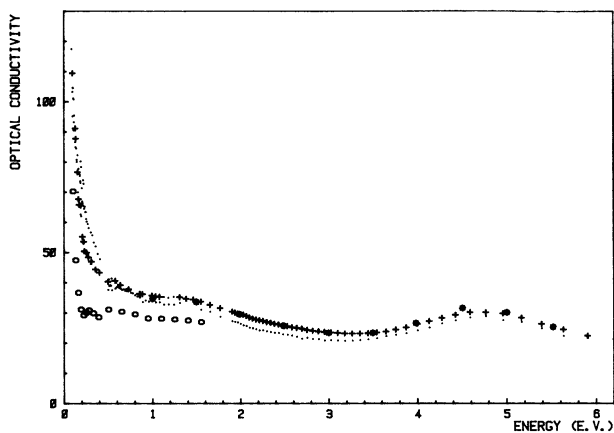

Fig. 6. — Complex dielectric function of Ni. 6a : real part ε_1. 6b : optical conductivity $\hbar\omega\varepsilon_2$. · our thin film. + Kramers-Kronig analysis on our thick films. ○ Lynch's results. * Stoll's results.

Table II. — *Drude parameters of* Ni *(ω_p = plasma frequency, $\hbar/\tau$ = relaxation time) as deduced from A.T.R. method, Kramers-Kronig analysis, Lenham* [13] *and Lynch* [5] *results.*

	A.T.R.	K.K.	Lenham	Lynch
(eV)	5.741	5.24	5.23	5.23
(eV)	0.051 (B = 1.6)	0.094 (B = 2.99)	0.058	0.056

We have introduced a frequency dependent relaxation time of the conduction electrons :

$$1/\tau_e = 1/\tau_0 + B\omega^2 .$$

This gives a better account of our results and is in agreement with more fundamental considerations about the shape of the Fermi surface of transition metals. In contrast to noble metals, the Fermi surface is no longer spherical but exhibits several bulges touching the Brillouin zone in many points. This leads to different types of carriers with different masses and relaxation times which can be taken into account in the Drude formulation by the introduction of a frequency dependent relaxation time. Other effects like electron-electron interaction can also induce such a variation but their influence, in this case, must be negligible compared to the Fermi surface anisotropy effect.

As it can be seen on the results (Tab. II), the $B\omega^2$ correction is relatively important, even at low energy, with respect to the constant term $1/\tau_0$. The calculation of a mean free path (or an optical conductivity) for the conduction electrons is thus meaningless since the relaxation time has lost its purely spatial physical meaning.

After subtraction of the Drude contribution, calculated above, from the total dielectric function $\tilde{\varepsilon}$, the absorption edge appears located between 0.11 and 0.15 eV (Fig. 6), in good agreement with the prediction of the Argand diagram. This result is also in total agreement with Kirillova's observations [7].

4.3 Interband transitions. — The main features already observed on the total absorption curves (Fig. 6) now clearly show up in figure 8.

All the curves (for both thin and thick films) exhibit a broad, roughly symmetrical peak centred at 4.7 eV (0.25 μm). This peak can be attributed to transitions from the bottom of the d band to empty states close to the Fermi level in different points of the Brillouin zone. This assumption seems more realistic than transitions between conduction bands ($L_2 \rightarrow L_1$) involving states well beyond E_F. It is in agreement with the predictions of band structure calculations, which estimate a band width of about 4.5 eV [8], but not with the results of angle-resolved photoemission experiments, which yield a narrower d-band, of the order of 3.3 eV [9].

A second well marked structure is observed at 1.4 eV; it is more dependent on the crystallite size : the smaller the crystallites, the weaker the structure.

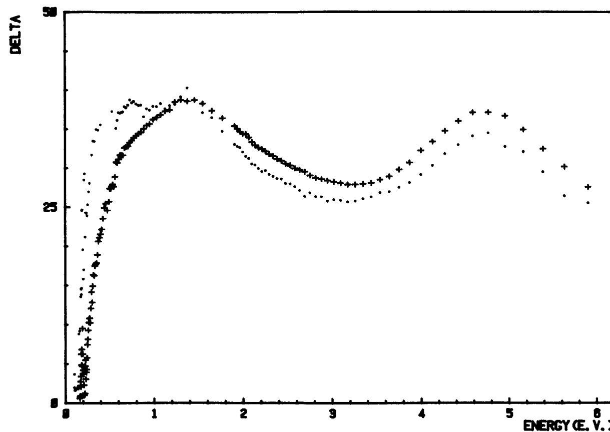

Fig. 8. — Interband optical conductivity Delta = $\hbar\omega\varepsilon_2$ (total) – $\hbar\omega\varepsilon_2$ (Drude) of Ni. · Our thin films. + Kramers-Kronig analysis on our thick films.

A similar structure has also been observed on different samples by different techniques [10, 8, 6]. Two interpretations have been proposed. The first one assigns the 1.4 eV peak to transitions between Q_+ and Q_- at the Fermi level (in the vicinity of the L point) [10, 11, 6], the other one to transitions between bands near the W symmetry point [8, 12]. Our measurements do not provide any additional information which could allow to distinguish between these two models.

Weak shoulders can also be noticed between 0.8 and 0.4 eV, which can be related to the features already pointed out by Kirillova [7] and by Stoll *et al.* [6]. They are also quite sensitive to the film structure. A clear interpretation of these low-energy absorptions is difficult since they may result from a variety of interband transitions, involving states close to E_F which are likely to be strongly affected by the magnetization state of the samples.

5. Conclusion.

We have presented a direct determination of the complex dielectric function of evaporated thin Ni films, in the infrared region, using the excitation of surface plasmon waves at the metal/air interface. This method, which requires accurate reflectivity measurements as a function of incidence, could be performed with the help of a specially designed infrared spectrophotometer. The results have been compared to those obtained by a Kramers-Kronig analysis of the reflectance of thick evaporated samples. The two methods are in good agreement, slight differences appearing only between the absolute values of $\tilde{\varepsilon}$.

Reliable values of the complex dielectric function of Ni are thus obtained over a large spectral range : 0.03 to 6 eV. They allow to determine the characteristic parameters of the conduction electrons, as well as the interband transition onset and the energies of the main features of the optical absorption, related to specific interband transitions. The results are in good agreement with those already obtained by Lenham [13], Lynch [5], Kirillowa [7], Stoll [6] and Ehrenreich [10], over more limited spectral ranges, on samples prepared by different methods.

Acknowledgments.

We wish to thank Marie-Luce Thèye for helpful comments, suggestions and careful reading of the manuscript.

References

[1] Abelès, F., *Advanced Optical techniques*, Ed. A. C. S. van Heel (North-Holland Publ. Co. Amsterdam) 1967, p. 145.

[2] Lafait, J., *J. Phys.* **F 8** (1978) 1597.

[3] Kretschmann, E., *Z. Phys.* **241** (1971) 313.

[4] Bouchard, M. G., *Proc. Int. Symp. on Basic Problems in Thin Film Physics*, Clausthal ed. R. Niedermayer and H. Mayer (Göttingen : Vanderhoeek and Ruprecht) 1966, p. 301.

[5] Lynch, D. W., Rosei, R., and Weaver, J. H., *Solid State Commun.* **9** (1971) 2195.

[6] Stoll, M. Ph. and Jung, C., *J. Phys.* **F 9** (1979) 2491.

[7] Kirillova, M. M., *Sov. Phys. J.E.T.P.* **34** (1972) 178.

[8] Shiga, M. and Pells, G. P., *J. Phys.* **C 2** (1969) 1847.

[9] Eastman, D. E., Himpsel, F. J. and Knapp, J. A., *Phys. Rev. Lett.* **40** (1978) 1514.

[10] Ehrenreich, H., Philipp, H. R. and Olechna, D. J., *Phys. Rev.* **131** (1963) 2469.

[11] Hanus, J., Feinleib, J. and Scouler, W. J., *Phys. Rev. Lett.* **19** (1967) 16.

[12] Hanus, J., Feinleib, J. and Scouler, W. J., *J. Appl. Phys.* **39** (1968) 1272.

[13] Lenham, A. P. and Treherne, D. M., Proceedings of the International Colloquium on *the Optical Properties and Electronic Structure of Metals and Alloys* (North-Holland Publishing Co., Amsterdam) 1966.